**Advances in
Geosciences**

Stord Orographic Precipitation Experiment (STOPEX): an overview of phase I

J. Reuder[1], **G. O. Fagerlid**[1], **I. Barstad**[2], and **A. Sandvik**[2]

[1]Geophysical Institute, University of Bergen, Norway
[2]Bjerknes Centre for Climate Research, Bergen, Norway

Abstract. STOPEX (Stord Orographic Precipitation Experiment) is a research project of the Geophysical Institute, University of Bergen, Norway, dedicated to the investigation of orographic effects on fine scale precipitation patterns by a combination of numerical modelling and tailored measurement campaigns. Between 24 September and 16 November 2005 the first field campaign STOPEX I has been performed at and around the island of Stord at the west coast of Norway, about 50 km south of Bergen. 12 rain gauges and 3 autonomous weather stations have been installed to measure the variability of precipitation and the corresponding meteorological conditions. This paper gives an overview of the projects motivation, a description of the campaign and a presentation of the precipitation measurements performed. In addition, the extreme precipitation event around 14 November with precipitation amounts up to 240 mm in less than 24 h, is described and briefly discussed. In this context preliminary results of corresponding MM5 simulations are presented, that indicate the problems as well as potential improvement strategies with respect to modelling of fine scale orographic precipitation.

1 Introduction

As moist air is forced over mountains, orographic precipitation (OP) is formed (e.g. Smith, 1979; Jiang, 2003). The phenomenon has miscellaneous and partly grave implications on the environment. Eroded landscapes and fresh water supply are two examples of environmental impact by OP. Hazardous events such as mudslides, avalanches and flooding, killing numerous of people every year, are strongly related to OP. In the climate system, the phenomenon is essential in maintenance and development of glaciers and the balance of fresh water, as well as for long-term trends in terrain evolution and the variation of plant and animal life.

The main mechanism of OP is the terrain induced forced lifting of air masses. The resulting horizontal precipitation pattern depends critically on various atmospheric parameters, as the speed and direction of the flow towards the mountain, the available moisture, and the stability of the approaching air. In addition the shape and dimension of the orographic barrier plays an important role. The spillover effect (e.g. Sinclair et al., 1996), i.e. the transport of rain droplets mainly created in the upwind lifting and condensation region into the lee in the presence of strong winds, is an integral manifestation of all parameters mentioned above. Combining flow dynamics, thermodynamics and cloud microphysics, this phenomenon provides a challenging test for model parameterization schemes. Recent studies (e.g. Zängl, 2005; Colle, 2004; Roe and Baker, 2005) have mainly focussed on modelling of OP associated to a typical halfwidth of the mountain barrier of 20 to 50 km. In the paper presented here we will emphasize to a somewhat smaller scale in the order of 5 to 10 km.

Norway (Fig. 1) with its steep mountains located in the belt of extra-tropical cyclone bringing moisture from lower latitudes, is an ideal test area for OP's impact. Due to its exposure to open ocean and the high frequency of extra-tropical cyclones approaching the area, in particular the western coast provides an excellent opportunity to study OP with high probability of detection.

We will present an overview of the measurements performed during the campaign STOPEX I. This campaign is intended to improve our understanding in fine scale orographic precipitation patterns by combination of model simulations and analysis of measurements.

Correspondence to: J. Reuder
(joachim.reuder@gfi.uib.no)
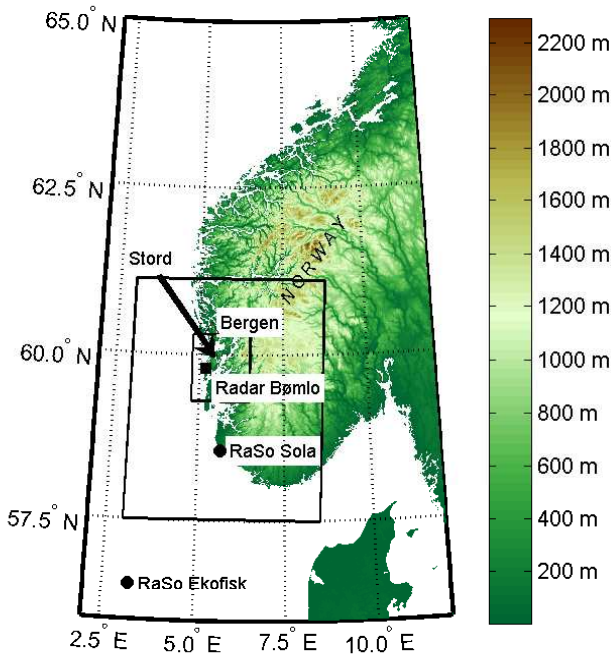
2 Campaign STOPEX I

2.1 Motivation

The island of Stord, located to the south of the city Bergen
at the west coast of Norway, has been the focus area for the
campaign (Fig. 2). The island extends about 30 km north-
south and 10 km east-west and its highest mountains form a
plateau at around 600 m. Climatological recordings of pre-
cipitation on the windward and the leeward side of the is-
land indicate a large horizontal gradient that has to be as-
sociated with orographic effects. On the eastern, predom-
inantly leeward side, Børtveit shows an annual average of
2661 mm during the 1931–1960 climatological period, while
Fitjar 10 km further upstream merely reaches a mean value
of 1590 mm per year.

The theoretical work of Smith and Barstad (2004) and the
corresponding observational assessment (Barstad and Smith,
2005) have been the initial motivation of this field campaign.
Observations from existing campaigns do not give a clear
view of how well the theory works. Particularly, information
on the natural time scale of OP related processes is needed.
The formation of hydrometeors in OP depends on the time
the droplets stay in an environment favorable for condensa-
tional growth, mainly in the windward lifting zone. Advec-
tion can transport these droplets to evaporation zones, partic-

Table 1. List of rain gauges (P1-P12) and weather stations (AWS1-AWS3) during STOPEX I.

	name	latitude deg N	longitude deg E	altitude [m]
P1	Korsvik	59.868	5.295	33
P2	Hovåsen	59.860	5.369	177
P3	Ytste Sørlivatnet	59.867	5.407	242
P4	Store Tjødnadalen	59.874	5.454	551
P5	Stemmetjødno	59.880	5.464	504
P6	Utløp Strupen	59.890	5.484	338
P7	Børtveitdalen	59.896	5.490	282
P8	Børtveit	59.889	5.520	10
P9	Nord-Huglo	59.864	5.570	32
P10	Lundastølen	59.843	5.480	187
P11	Kattnakkjen	59.875	5.494	697
P12	Vistvik	59.944	5.413	104
AWS1	Nautøy	59.737	5.386	2
AWS2	Kattnakkjen	59.874	5.493	700
AWS3	Korsneset (Nord-Huglo)	59.824	5.573	3

ularly in the lee, where number and size of droplets will de-
crease. The observational indications from Stord have shown
that this site is promising for studies of these mechanisms.

Guidance for the campaign design was provided by the
theory, first of all by running a linear model in a quasi-steady
operational modus for 3 months upfront of the campaign. It
was decided to deploy rain gauges ("tipping-buckets") where
the theory indicated the strongest gradients, and see if the
gradient changed dramatically for different weather regimes.
The gauges have been aligned across and along the highest
mountains (P1-P12 in Fig. 2). The gauge at P2 failed after
short operation, therefore only 11 precipitation data series are
available for evaluation. At one location, three collectors (P4,
P5, P6) have been located within a distance below 2 km at
comparable elevation to test if the collectors capture the same
precipitation signal. In addition three autonomous weather
stations (AWS1-AWS3) recording 10 min averages of wind,
temperature and humidity have been deployed. They were
partly used to see if channelling effects around the island
could explain some of the variation in precipitation. Their
location is also indicated in Fig. 2.

2.2 Instrumentation

For the precipitation measurements the data logging rain
gauge HOBO RG2 has been used. The instruments are
based on the tipping bucket principle and enable a resolu-
tion of 0.2 mm. The rain gauges have been validated by a
three month intercomparison campaign from May to August
2005. For that two of the 12 HOBO rain gauges (serial num-
bers 20371 and 20372) have been operated in parallel to the
official precipitation registration performed by the Norwe-
gian Meteorological Service (met.no) at the station Bergen-
Florida based on standard rain gauge measurements.

The monthly integrated precipitation amount of both HOBO instruments coincides within ±0.5%. Compared to the measurements of met.no the RG2 gauges underestimate monthly integrated precipitation slightly by 2% (June) to 6% (May). A closer look into daily integrated values shows that the underestimation mainly occurs for small precipitation amounts below 5 mm/day. This behavior can most likely be addressed to the protective grating of the HOBO instrument. It is intended to minimize blocking of the rain gauge by e.g. falling leaves or insects. Of course it also provides an additional surface area that increases losses in measured precipitation by the effects of surface wetting and evaporation. These effects are strongest for weak and intermittent precipitation events.

The meteorological measurements at the three selected sites have been performed by autonomous weather stations (AWS) of Aanderaa Data Instruments (AADI). Each of the stations has been equipped with sensors for temperature, relative humidity, wind speed, and wind direction.

2.3 Measurements

The measurements of STOPEX I cover the time period between 24 September and 16 November 2005. During the campaign, 21 different precipitation events have been identified with respect to the large scale synoptic situation, derived from surface and 500 hPa analysis charts and infrared satellite images. An overview is given in Table 2. For each identified period the table provides a short description of the synoptic situation, the range of observed accumulated precipitation at the stations P1 to P12, and the average surface temperature measured at the AWS3 Huglo-Korsneset. From radiosonde ascents at Sola, about 150 km south of Stord, wind speed and wind direction at the 925 hPa level have been used to characterize the large scale flow conditions. The soundings available every 12 h have been selected with respect to best representation of the period of maximum precipitation during each event. In addition two stability parameters N_d and N_m for the atmospheric boundary layer have been calculated from the sounding data at the surface and the 850 hPa level:

$$N_d = \delta \sqrt{\left| \frac{g_0}{\theta} \frac{d\theta}{dz} \right|} \qquad N_m = \delta \sqrt{\left| \frac{g_0}{\theta_e} \frac{d\theta_e}{dz} \right|} \qquad (1)$$

g_0 : gravity
θ : potential temperature
θ_e : equivalent potential temperature
z : altitude
δ : stability indicator (+1: stable; −1: instable)

N basically represents a slightly modified version of the Brunt-Vaisala frequency for dry- and moist-adiabatic conditions, with negative values (instead of imaginary numbers) indicating instability. The magnitude of both stability parameters or a combination of them are expected to provide a
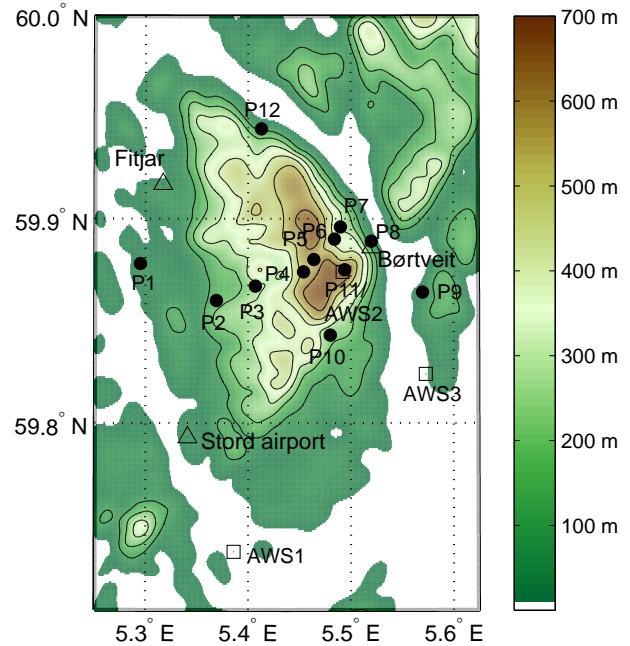
Fig. 2. Topography of Stord with location of rain gauges (P1-P12) and autonomous weather stations (AWS1-AWS3) during the field campaign STOPEX I. At Stord airport continuous routine observations are performed by the Norwegian Meteorological Service met.no.

measure for the classification of the identified precipitation events into stratiform, convective and mixed cases.

During the 8 week campaign a total amount of precipitation between 340 mm (P1: Korsvik, 30 m a.s.l.) and 1237 mm (P11: Kattnakkjen, 697 m a.s.l.) has been observed (Fig. 3). It has to be mentioned that these precipitation values have not been corrected with respect to the known decrease in sample efficiency with increasing wind speed (e.g. WMO, 1998; Nespor and Sevruk, 1999). Due to the measurement height of around 1 m above ground, and the shielded surrounding of some of the rain gauges, the wind effects should not be too dramatic, but they will tend to increase the measured values especially for the higher and therefore more wind exposed sites.

Figure 4 shows that the precipitation in general increases markedly with altitude. In addition the data indicate that the stations on the leeward side of Stord (P6 to P9) receive distinctly higher precipitation amounts then those at corresponding altitudes on the windward side. P6 and P7, located around 300 m, reach values comparable to P4 and P5, elevated above 500 m on the windward side of the mountains. Compared to the westernmost site P1 close to sea level, the two leeward measurements at comparable elevation (P8, P9) registered more than twice in total amount of precipitation. This feature is a typical manifestation of the spillover effect.

Table 2. Overview of precipitation events during STOPEX I. Values given for each period are the range of accumulated precipitation (P) measured by the rain gauges, the 925 hPa wind speed and wind direction from sounding at Sola, the stability as modified (negative values indicate instable conditions) Brunt-Vaisala frequencies (N_d and N_m) calculated from potential temperature θ and equivalent potential temperature θ_e between surface and 850 hPa , and the average temperature (T_0) measured at Huglo-Korsneset. The soundings available every 12 h have been selected with respect to be representative for the period of maximum amount of precipitation during each event.
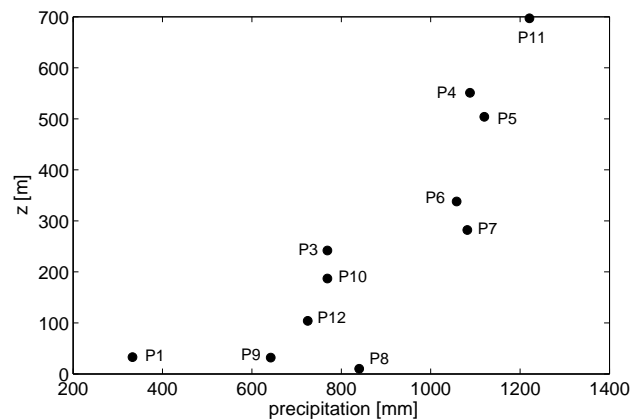
#	time interval	synoptic situation	P [mm]	vv [m s^{-1}]	dir	N_d/N_m [$\times 10^{-2}$s^{-1}]	T_0 [degC]
1	27.09. 00–28.09. 12	cold front and showers behind	11–48	24	S	1.25/−1.35	13
2	28.09. 12–30.09. 00	several occlusions	20–42	9	SW	0.93/−0.50	10
3	30.09. 09–02.10. 03	frontal system	14–81	18	S	1.03/−0.30	13
4	02.10. 09–04.10. 03	occlusion	7–39	4	W	0.88/−0.75	11
5	08.10. 18–09.10. 18	sharp cold front with few subsequent showers	20–37	21	SSE	1.45/0.74	10
6	12.10. 18–14.10. 12	cold front and subsequent showers	17–60	23	SSE	1.25/−0.60	13
7	20.10. 00–23.10. 00	several fronts/occlusions; rather complicated situation	35–115	11	SSW	0.70/−1.08	11
8	25.10. 00–27.10. 00	occlusion and warm front, close to center of low	14–60	30	SE	1.47/1.34	6
9	28.10. 12–29.10. 00	cold front	12–33	28	S	1.28/0.12	13
10	30.10. 09–31.10. 06	cold front	3–28	20	S	1.32/0.85	14
11	31.10. 15–01.11. 06	cyclogenesis at stationary front	8–20	21	SSE	1.33/0.94	12
12	30.10. 09–31.10. 06	passage of cold front and 2 subsequent troughs	5–32	15	S	1.10/−0.33	11
13	02.11. 12–04.11. 00	occlusion and subsequent trough	14–56	19	SSE	1.46/1.13	12
14	04.11. 00–05.11. 00	occlusion	18–84	14	S	1.36/0.90	12
15	05.11. 12–06.11. 09	occlusion	1–17	10	SSW	1.17/0.41	10
16	06.11. 12–08.11. 00	warm front, cold front, trough	8–48	18	SSW	1.52/1.21	11
17	08.11. 00–09.11. 18	passage of frontal system, cyclogenesis	43–86	25	SSW	1.12/0.02	13
18	10.11. 00–11.11. 06	occlusion and subsequent showers	15–44	–	–	–	10
19	11.11. 03–12.11. 03	passage of warm and cold front	3–26	13	S	1.20/0.71	11
20	12.11. 03–13.11. 12	occlusion, cyclogenesis	8–53	14	W	0.96/−0.49	10
21	13.11. 21–15.11. 15	passage of frontal system, subsequent showers	45–240	14–25	SW–W	1.18/0.76	10
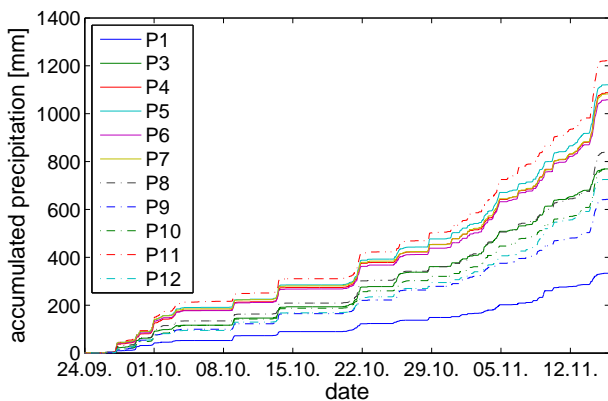
Fig. 3. Accumulated precipitation during the 8 week campaign of STOPEX I.

**Fig. 4.** Altitude dependence of accumulated precipitation during the 8 week campaign of STOPEX I.

3 Case study: Extreme precipitation event 13–15 November 2005

During 14 November the fronts of a low pressure system pass southern Norway and lead to exceptionally high precipitation amounts along the Norwegian coast. On 12 November 00:00 UTC, the cyclone is already well developed and its center (986 hPa) is located around 60° N at the east coast of Newfoundland. Between it and a strong anticyclone over the central North Atlantic, subtropical moist air is transported towards North. Until 13 November 00:00 UTC the cyclone has slightly weakened (1001 hPa) and moved in between Greenland and Iceland. During the next 24 h the system is
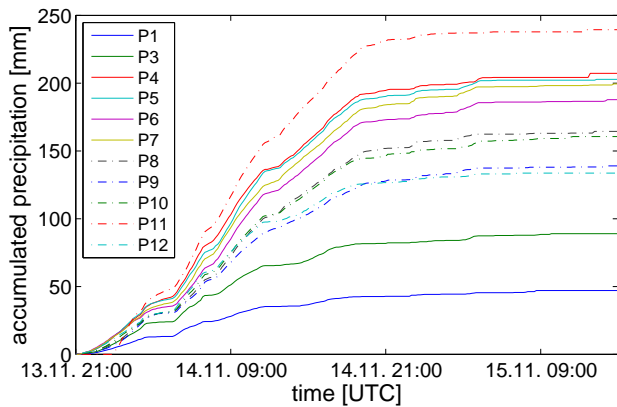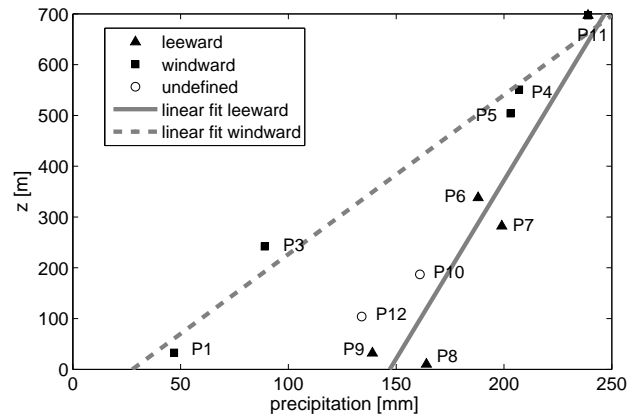
Fig. 5. Accumulated precipitation during event 21 of STOPEX I. For extended legend see Fig. 3.

Fig. 6. Altitude dependence of accumulated precipitation during event 21 of STOPEX I.

intensifying vigorously (14 November 00:00 UTC: 976 hPa), steadily advecting moist subtropical air.

3.1 Measurements

The precipitation field associated with this frontal system reaches Stord on 13 November around 22:00 UTC (Fig. 5). Within a 24 h period, precipitation amounts between 45 mm (P1: Korsvik) and 240 mm (P11: Kattnakkjen) are measured by the STOPEX rain gauge network. A closer look into the time series of accumulated precipitation reveals four distinct periods of high, nearly constant precipitation intensity, indicated by nearly linear and steep increase in accumulated precipitation. These intense precipitation periods, typically lasting 3 to 5 h are separated by shorter (lasting typically 1–2 h) phases of distinctly lower precipitation intensities. This temporal structure is occurring nearly simultaneously at all rain gauges and can therefore not be related to local orography. Explanation for these fluctuations must therefore rather be connected to large scale fluctuations.

Figure 6 presents the altitude dependence of the accumulated precipitation during event 21 from 13.11.2005 21:00 UTC until 15.11.2005 15:00 UTC. This event was characterized by quite strong wind (10 min averages measured at AWS3: 15–25 m/s), at the beginning from Southwest, later from West. The selected positions of rain gauges oriented along the mean incoming flow of moist air (except P10 and P12) provide therefore an ideal transect for the investigation of this precipitation event. The measured precipitation amounts show again a distinct increase with altitude. By separating windward (P1-P5) and leeward stations (P6-P9), two different regimes of altitude dependence of the precipitation amount become evident. Obviously both regimes can be approximated by a linear dependency with height indicated by the fitted curves in Fig. 6. The distinctly larger gradients are observed windward, with an increase of nearly

200 mm per 700 m, i.e. nearly fourfold precipitation amount at P11 compared to P1. The fit through the data of the leeward stations results in an increase of around 100 mm per 700 m (from appr. 150 to 250 mm). The leeward stations close to sea level receive around 150 mm about, i.e. approximately the threefold precipitation amount of P1 upstream. This again can only be explained by the spillover effect already mentioned above.
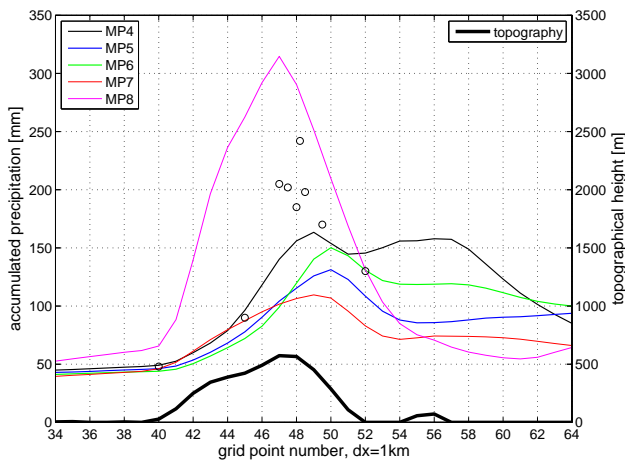
3.2 Model simulations

In a first attempt, numerical sensitivity experiments for the event 21 have been performed with the mesoscale atmospheric model MM5 version 3.6 (see Dudhia, 1993; Grell et al., 1994, or http://www.mmm.ucar.edu/mm5/ for details). The model has been configured with four domains, the outermost covering the southern part of Norway, the North Sea and parts of the Norwegian Sea, the innermost covering the island of Stord and its surroundings. The two inner domains D3 and D4 are shown as boxes in Fig. 1. The horizontal grid resolutions have been selected as 27, 9, 3 and 1 km, the corresponding modelling time steps are 81, 27, 9 and 3 s. Each numerical simulation started on November, 13:00 at 12:00 UTC and lasted for 30 h. The model has been initialized with analyzes of upper air and surface data from ECMWF, and lateral boundary values have been included every 6 h during the simulation. Model output data for further analysis have been taken every hour.

Sensitivity experiments with 5 different microphysical parameterizations schemes given in Table 3 have been performed. The radiation transfer has been treated by the Dudhia radiation scheme (Dudhia, 1993). The Grell convection parameterization (Grell et al., 1994) has been used for the 27 km domain, while convection is assumed to be solved explicitly for the higher horizontal resolutions. Turbulence is parameterized by the MRF scheme (Hong and Pan, 1996).

Table 3. Microphysical parameterization schemes used for MM5 simulations.

abbreviation	scheme	reference
MP4	simple ice	Dudhia (1993)
MP5	Reisner 1 microphysics	Reisner et al. (1998)
MP6	Goddard microphysics	Lin et al. (1983), Tao et al. (1989), Tao and Simpson (1993)
MP7	Reisner 2 microphysics	Reisner et al. (1998), Thompson et al. (2004)
MP8	Schultz microphysics	Schultz (1995)

Fig. 7. MM5 simulations of accumulated precipitation along a transect across Stord for the period 13 September 12:00 UTC until 14 September 18:00 UTC using five different cloud microphysics parameterization schemes. The bold solid line represents the MM5 model topography. Circles denote corresponding observations of the rain gauge network.

The occurring differences in total precipitation amount and in the spatial distribution amongst the model runs confirm the need of appropriate precipitation measurements for validation purposes. Measured accumulated precipitation values for the event 21 from the rain gauges P1 to P9, located close to the transect, have been plotted as open circles in Fig. 7. Excellent agreement between measurements and MP4 to MP7 simulations can be found at the windward side of Stord. In contrast to the results of these simulations the measured maximum of precipitation coincides with the maximum of topography. Moreover the measured values are markedly above the simulated ones at these elevations. Due to the fact that the measurements have not been corrected with respect to wind-induced undersampling, the real measured values should tend to be even higher. In the lee of the island measurements and model results seem to converge again. Based only on one measurement, this fact should not be overinterpreted. Anyway, the model simulations point out that for future validation purposes additional rain gauges have to be deployed in the downstream region.

4 Summary and Outlook

During STOPEX I high resolution time series of precipitation have been derived from rain gauge measurements at 11 sites on and around the island of Stord. These measurements represent an unique data set on horizontal fine-scale variability of OP. The data presented here preliminarily, will be used in the future for extended comparison and validation tasks of OP model simulations both using advanced weather prediction models (e.g. MM5) as well as simpler process oriented models, like the linear model of OP proposed by Smith and Barstad (2004). Due to its high temporal resolution the presented data set can not only be used for comparing daily amounts of precipitation, as mostly done in the past. These data now enable moreover the validation of simulated precipitation intensities and have thus a large potential to increase our understanding of the underlying microphysical processes.

In addition this first campaign has given invaluable information for the redistribution and extension of the rain gauge network for the forthcoming, extended campaign STOPEX II

The results of the model simulations along a transect across Stord are presented in Fig. 7. Except the Schultz microphysics scheme MP8 the MM5 results agree reasonable for the windward side of Stord. Approaching the highest part of the mountains, the deviations between these schemes increase. The maxima of predicted precipitation are slightly shifted to the lee and range between 125 mm and 165 mm for the simulated 30 h period. Further downstream the differences between the different schemes reach a maximum (MP4: 160 mm; MP 7: 75 mm) before obviously converging again about 15 km downstream the top of the orography. In contrast the Schultz scheme MP8 shows a completely different behavior. It already starts with slightly enhanced precipitation when approaching the island. Reaching the coast line the amount of precipitation increases sharply to a maximum of more than 310 mm that is allocated exactly above the highest topography. In the lee the accumulated precipitation decreases with distance nearly as steep as it increased upstream.

during autumn 2006. At least 6 additional rain gauges will be deployed and a recently purchased Micro Rain Radar (MRR by Metek) will be available both for stationary and mobile precipitation measurements. Additional sources of information (e.g. integrated water vapor from dual band GPS measurements (e.g. Bevis et al., 1992) and high resolution precipitation information derived from the mobile phone transmitter network (Messer et al., 2006) will complement our own measurements during STOPEX I and STOPEX II.

References

Barstad, I. and Smith, R. B.: Evaluation of an orographic precipitation model, J. Hydrometeorol., 6, 85–99, 2005.

Bevis, B. G., Bussinger, S., Herring, T. A., Rocken, C., Anthes, R. A., and Ware, R. H.: GPS meteorology: Remote sensing of atmospheric water vapor using the Global Positioning System, J. Geophys. Res., 97, 15 787–15 801, 1992.

Colle, B. A.: Sensitivity of orographic precipitation to changing ambient conditions and terrain geometries: An idealized modeling perspective, J. Atmos. Sci., 61, 588–606, 2004.

Dudhia, J.: A nonhydrostatic version of the Penn State NCAR Mesoscale Model – Validation tests and simulation of an Atlantic cyclone and cold-front, Mon. Wea. Rev., 121, 1493–1513, 1993.

Grell, G., Dudhia, J., and Stauffer, D.: A Description of the Fifth-Generation Penn State/NCAR Mesoscale Model (MM5), National Centre for Atmospheric Research, Boulder Colorado, US, 1994.

Hong, S.-Y. and Pan, H.-L.: Non-local boundary layer vertical diffusion in a medium-range forecast model, Mon. Wea. Rev., 124, 2322–2339, 1996.

Jiang, Q.: Moist dynamics and orographic precipitation, Tellus, 55A, 301–316, 2003.

Lin, Y.-L., Farley, R. D., and Orville, H. D.: Bulk parameterization of the snow field in a cloud model, J. Clim. Appl. Meteorol., 22, 1065–1092, 1983.

Messer, H., Zinevich, A., and Alpert, P.: Environmental monitoring by wireless communication networks, Science, 312, 713, 2006.

Nespor, V. and Sevruk, B.: Estimation of wind-induced error of rainfall gauge measurements using a numerical simulation, J. Atmos. Ocean. Tech., 16, 450–464, 1999.

Reisner, J., Rasmussen, R. M., and Bruintjes, R. T.: Explicit forecasting of supercooled liquid water in winter storms using the MM5 mesoscale model, Q. J. R. Meteorol. Soc., 124, 1071–1107, 1998.

Roe, G. H. and Baker, M. B.: Microphysical and geometrical controls on the pattern of orographic precipitation, J. Atmos. Sci., 63, 861–880, 2005.

Schultz, P.: An explicit cloud physics parameterization for operational numerical weather prediction, Mon. Wea. Rev., 123, 3331–3343, 1995.

Sinclair, M. R., Wratt, D. S., Henderson, R. D., and Gray, W. R.: Factors affecting the distribution and spillover of precipitation in the Southern Alps of New Zealand – A case study, J. Appl. Meteorol., 36, 428–442, 1996.

Smith, R. B.: The influence of mountains on the atmosphere, Adv. Geophys., 21, 87–230, 1979.

Smith, R. B.: A linear time-delay model of orographic precipitation, J. Hydrol., 282, 2–9, 2004.

Smith, R. B. and Barstad, I.: A linear theory of orographic precipitation, J. Atmos. Sci., 61, 1377–1391, 2004.

Tao, W.-K., Simpson, J., and McCumber, M.: Ice-water saturation adjustment, Mon. Wea. Rev., 117, 231–235, 1989.

Tao, W.-K. and Simpson, J.: Goddard Cumulus Ensemble Model. Part I: Model description, Terr. Atmos. Ocean. Sci., 4, 192–209, 1993.

Thompson, G., Rasmussen, R. M., and Manning, K.: Explicit forecasts of winter precipitation using an improved bulk microphysics scheme. Part I: Description and sensitivity analysis, Mon. Wea. Rev., 132, 519–542, 2004.

WMO: WMO Solid Precipitation Measurement Intercomparison, WMO Instruments and Observing Methods, Report No. 67, WMO/TD 872, 1998.

Zängl, G.: The impact of lee-side stratification on the spatial distribution of orographic precipitation, Q. J. R. Meteorol. Soc., 131, 1075–1091, 2005.